Linking flow velocity-regulated EPS production with early-stage biofilm formation in drinking water distribution systems

Yanyan Liu, Rongrong Shan, Guowei Chen and Li Liu

ABSTRACT

Hydrodynamics impacts interactions between microbes and their micro-habitats in aqueous systems, thus the study of hydrodynamics is key to understanding the formation and dynamics of biofilms. Yet mechanisms of how microbial responses to hydrodynamics regulate biofilm formation in drinking water distribution systems (DWDS) are underappreciated. Here, we investigated the linkage between early-stage biofilm formation and flow velocity fluctuations in a model DWDS. Results showed that an intermediate velocity (1.0 m/s) enhanced biofilm formation, with the highest biofilm/total cells ratio of 96.91% ± 2.26%. Moreover, the intermediate velocity promoted extracellular polymeric substances (EPS) release, accompanied with lowered zeta potential and elevated hydrophobicity of suspended cells, which could be responsible for surface aggregation. Shifts in biofilm community were observed along with hydrodynamics fluctuations. Intermediate velocity (1.0 m/s) stimulated the dominance of *Proteobacteria* (78.16%) along with the genus predominance of *Pseudomonas*, known to secrete large amounts of EPS favoring biofilm formation. Overall, this study provides new understanding of biofilm formation responding to hydrodynamic fluctuations in DWDS.

Key words | bacterial community, biofilm formation, drinking water distribution systems, EPS, flow velocity

Yanyan Liu
Rongrong Shan
Guowei Chen
Li Liu (corresponding author)
School of Civil Engineering,
Hefei University of Technology,
Hefei 230009,
China
E-mail: *lliu@hfut.edu.cn*

INTRODUCTION

Populating harsh and dynamic environments, microbes, including bacteria, fungi and archaea, are prone to colonize on pipeline surfaces to form biofilms in drinking water distribution systems (DWDS) (Douterelo *et al.* 2014; Potgieter *et al.* 2018). The occurrence of surface-associated biofilms can deteriorate the distributed water quality with associated undesirable turbidity or odors (Fish *et al.* 2017), operation malfunction (Zacheus *et al.* 2001; Bertelli *et al.* 2018), the spread of pathogens and antibiotic resistant bacteria (Zhang *et al.* 2018). The DWDS often suffer from hydrodynamic fluctuations from stagnant, laminar to turbulent flow regimes, which intensifies the numerous localized biophysical interactions between individual cells and their micro-habitats (Stoodley *et al.* 1999; Purevdorj *et al.* 2002; Guasto *et al.* 2012; Douterelo *et al.* 2016; Tsagkari *et al.* 2017; Tsagkari & Sloan 2018b). However, the knowledge about hydrodynamics-triggered biofilm formation in DWDS remains underappreciated.

Hydrodynamics serves as the most critical factor shaping distribution of nutrients, suspended particulates, dissolved oxygen and external physical stresses on biofilms, accordingly controlling the micro-habitats of microbes and impacting biofilm dynamics (Teodósio *et al.* 2011; Lemos *et al.* 2015; Fish *et al.* 2017). For example, increasing flow velocity was observed to result in lower cell numbers per unit surface area due to higher biofilm detachment by elevated

doi: 10.2166/ws.2020.039

shear stress in a simulated DWDS (Manuel *et al.* 2007). In contrast, Raya *et al.* (2010) found that augmenting flow velocity yielded an increasing-then-decreasing trend of the extent of *Pseudomonas aeruginosa* PAO1 attachment onto clean and smooth surfaces, which may be attributed to the combined effects of hydrodynamics-evoked shear stress and mass transfer. Shen *et al.* (2015) observed that local flow conditions created by biofilm roughness asperities altered *Legionella pneumophila* adhesion on the developed DWDS biofilm on account of enhanced interception. Meanwhile, it was also reported that a reduction in bacterial diversity occurred subject to high shear stress, reflective of its functions on slowing down biofilm maturation (Rochex *et al.* 2008).

Moreover, extensive studies have yielded significant insights into the linkages between hydrodynamics and cellular-induced reactions, including cell motility, nutrient uptake, proliferation, extracellular polymeric substances (EPS) production, and quorum sensing (O'Toole & Kolter 1998; Pratt & Kolter 1998; Harshey 2003; Kirisits *et al.* 2007; Picioreanu *et al.* 2007; Guasto *et al.* 2012; Kim *et al.* 2016; Tsagkari & Sloan 2018a). Among them, the presence of EPS is essential in the processes of adhesion to substratum surfaces and biofilm formation by promoting survival strategies such as cell attachment to surfaces, protective barrier and nutrient trapping (Flemming & Wingender 2010; Lorite *et al.* 2013). An increase in hydrodynamic shear has been shown to stimulate bacterial exopolysaccharide secretion (Liu & Tay 2002). However, the *Pseudomonas fluorescens* biofilms under different flow regimes expressed distinct physiological characteristics, where turbulent flow promoted formation of higher cell density biofilms with lower amounts of matrix polysaccharides than laminar flow that generated low shear stress (Simões *et al.* 2007). Fish *et al.* (2017) observed that the biofilms developed under low-varied flow conditions had the lowest amounts of biomass and the greatest EPS volumes per cell when compared with those incubated at greater flow variations in an experimental DWDS system. Despite these important advances, the underlying mechanisms of early-stage DWDS biofilm linked to hydrodynamics-stressed EPS production are not clear, which would help unravel the complexity of hydraulics regulation on biofilm dynamics.

This study examines how flow velocity fluctuations could affect early-stage DWDS biofilm formation through determining the changes in bacterial cells, EPS production and surface properties along with variations in biofilm bacterial community with the aim of enhancing our knowledge of biofilm formation processes in DWDS.

MATERIALS AND METHODS

Experimental systems and preparation

The experiments were carried out in a closed DWDS, as illustrated in Figure S1 (Supplementary Material), consisting of a 3 L tank and a 10 m polyethylene (PE) pipe (inner diameter of 6 mm), where removable pipe sections (4 cm long) were inserted in the middle for biofilm collection. The water flow and internal velocities of pipelines were driven through peristaltic pumps (Lange BT300-2 J, Lange BT600-2 J, Baoding, China) for low or high velocity conditions, respectively. The pipelines and biofilm collectors were rinsed with 70% ethanol and then the system was disinfected by flushing using 1.0 mg/L sodium hypochlorite solution for 2 h (Soini *et al.* 2002) prior to experiments. Water samples used in the experiment were collected from a domestic drinking water tap in Hefei, China, and stored at room temperature ($20 \pm 1\ ^{\circ}C$) for 24 h to diminish chlorine residual before use.

Experimental setup

To evaluate the impacts of flow velocity on early-stage biofilm formation, five parallel experimental systems were employed with various internal velocities of 0.1(laminar flow), 0.5 (transition flow), 1.0, 1.5, and 2.0 m/s (turbulent flow), respectively, mimicking the flow fluctuations regularly occurring in DWDS. At these velocities, the Reynolds numbers were 594, 2,970, 5,940, 8,910 and 11,880, respectively. Biofilm and bulk water samples were collected at 3 h, 6 h, 12 h, 24 h and 48 h after inoculation for estimating attached and suspended cell density, protein (PN) and polysaccharide (PS) contents, zeta potential and hydrophobicity of suspended cells, along with biofilm bacterial community analysis.

Biofilm and bulk water sampling

After wiping the outside surfaces with 70% ethanol, the biofilm collectors were gently washed three times with distilled

water to eliminate unattached cells (LeChevallier *et al.* 1988; Percival *et al.* 1998). The collectors were then aseptically put into a 15.0 mL sterilized tube preloaded with 10.0 mL of phosphate buffer saline (PBS). Sonication (KQ5200DE, Shumei, Kunshan, China) at 35 kHz for 10 min was conducted to gather the suspension of attached cells in the tube (Manuel *et al.* 2007). In the meantime, 30.0 mL of the water sample from the systems were transferred to a 50.0 mL sterile centrifuge tube for further analysis.

Bacterial cell enumeration

Heterotrophic plate counts (HPC) were enumerated by a spread plating method on R_2A-agar, where 100.0 μL sample or dilution from biofilm cell suspensions or bulk water were spread (Lehtola *et al.* 2006). The cultures were incubated at 22 °C for 7 d before enumerating colony forming units (CFU) (Lehtola *et al.* 2006). The acridine orange direct counts method was applied to determine total cell counts (TCC) (Lehtola *et al.* 2004). In detail, 5.0 mL of diluted cell suspension was filtered through a black 0.22 μm Nuclepore membrane filter (Whatman, Nuclepore, Clifton, NJ, USA), followed by staining with 12.5 μL of 0.01% acridine orange dilution. The total cells were counted using a fluorescence microscope (IX73, Olympus, Japan) with ten randomly selected spots from three replicates for each sample. To determine where cells were present, the attaching ratio (R_{att}) was estimated by the fraction of the cells present in biofilms relative to total cells in the system, described as follows (Srinivasan *et al.* 2008):

$$R_{att} = \frac{AX_{bio}}{(VX_{bulk} + AX_{bio})}$$

where A represents the surface area per unit length of pipe (cm^2), V is the volume per unit length of pipe (mL), X_{bio} is the concentration of biofilm cells (cells/cm^2), and X_{bulk} is the concentration of bulk water cells (cells/mL).

EPS, zeta potential and surface hydrophobicity analysis

Extracellular PS and PN were extracted from cell suspensions of biofilm and planktonic samples and analyzed via a modified heat method (Li & Yang 2007). Fifteen-millilitre cell suspension were transferred into a test tube and heated in a water bath at 70 °C for 1 h. Subsequently, the suspensions were sheared by a vortex mixer (CJ78-1, Jintan, China) for 1 min, followed by centrifugation at 4,000g (5804, Eppendorf, Germany) for 15 min. After filtrating the supernatant through 0.45 μm filters, PN and PS were quantified using a UV/VIS spectrophotometer (Unico, Shanghai, China) at 750 nm in accordance with Liu *et al.* (2017). The electrophoretic measurements of suspended cells were measured by a zeta-potential analyzer (Nano-ZS90, Malvern, UK). Surface hydrophobicity was estimated with the method developed by Rosenberg *et al.* (1980).

Staining and confocal laser scanning microscope imaging

A confocal laser scanning microscope (CLSM; LSM710, Carl Zeiss, Germany) was used to characterize the physical structure of the biofilm. Specifically, the biofilm collectors were cut into three strips (1.5 cm × 0.5 cm), then transferred to PBS solution, and stored at 4 °C until analyzed. The collectors were stained with 100.0 μL SYTO63 solutions (20 μmol/L, Thermo Fisher Scientific, OR, USA) and incubated for 30 min to bind to biofilm cells. Afterwards, proteins were stained with 100.0 μL FITC solution (10 g/L, Sigma, MO, USA) for 1 h. For α-polysaccharide staining, 100.0 μL Con A (250 mg/L, Thermo Fisher Scientific, OR, USA) was added and incubated for 30 min. Finally, 100.0 μL calcofluor white solution (300 mg/L, Sigma, MO, USA) was added and incubated for 30 min to bind to β-polysaccharide. After each staining, samples were rinsed three times with PBS and then allowed to dry naturally (Chen *et al.* 2007; Jiang & Liu 2013). The stained samples were visualized using a ×20 objective and analyzed with ZEN 2009 light edition confocal software.

Bacterial community analysis

The collected biofilm samples were placed into a 50.0 mL centrifuge tube containing sterile PBS (pH 7.0) and centrifuged at 4,000g for 5 min, followed by resuspension of the pellets. After repeating these steps three times, the total DNA extraction was performed using the E.Z.N.A Mag-Bind Soil DNA Kit (OMEGA, MO BIO Lab. Inc., Carlsbad, CA, USA) according to the manufacturer's instructions.

The high-variation region of the 16S rRNA gene was subjected to polymerase chain reaction (PCR) amplification using universal primers (F-27FAGAGTTTGATCMTGGC TCAG) and (R2-CAAGTATTACCGCGGCTGCTGGCAC), and the V1–V3 regions were selected as the amplification regions. PCR products were pooled and purified using the Qubit2.0 DNA detection kit (Qubit® ss DNA Assay Kit, Life Technologies). Biofilm bacterial communities and their relative abundance and diversity were analyzed by a high-throughput sequencing method (pyrosequencing) (Douterelo *et al.* 2012), which was conducted by Sangon Biotech Company (Sangon, China) with the Illumina Miseq platform (Illumina, Inc., San Diego, CA, USA). The sequence-similarity-based method was used to classify the sequences into different operational classification units at 97% similarity level using QIIME software.

Statistical analysis

All experiments were conducted at least in triplicate and the results were presented with average and standard deviations. Statistical differences were analyzed with the one-way analysis of variance (ANOVA) test, which was based on a confidence level equal to or higher than 95%. The Pearson correlation test was conducted to evaluate correlation coefficients (r) among EPS amounts, zeta potential, hydrophobicity and attaching ratios.

RESULTS AND DISCUSSION

Effects of flow velocities on biofilm formation and suspended-cell growth

Figure 1 depicts the HPC and TCC variations on pipe surfaces and in bulk water across various flow velocities. After 48 h incubation, significant differences ($p < 0.001$) were found in biofilm cell densities. A biofilm-embedded TCC of 4.88 ± 0.03 lg(cells)/cm^2 was estimated at the low velocity of 0.1 m/s (Figure 1(a)), which rose up to 6.05 ± 0.04 lg(cells)/cm^2 responding to 1.0 m/s velocity. Elevating the velocity to 2.0 m/s yielded a gradual drop of biofilm TCC to 5.44 ± 0.11 lg(cells)/cm^2. Correspondingly, an opposite significant effect of flow velocity on suspended-cell growth was observed compared with biofilm formation ($p < 0.001$). Specifically, the suspended cell population was estimated as decreasing in TCC value from 4.60 ± 0.01

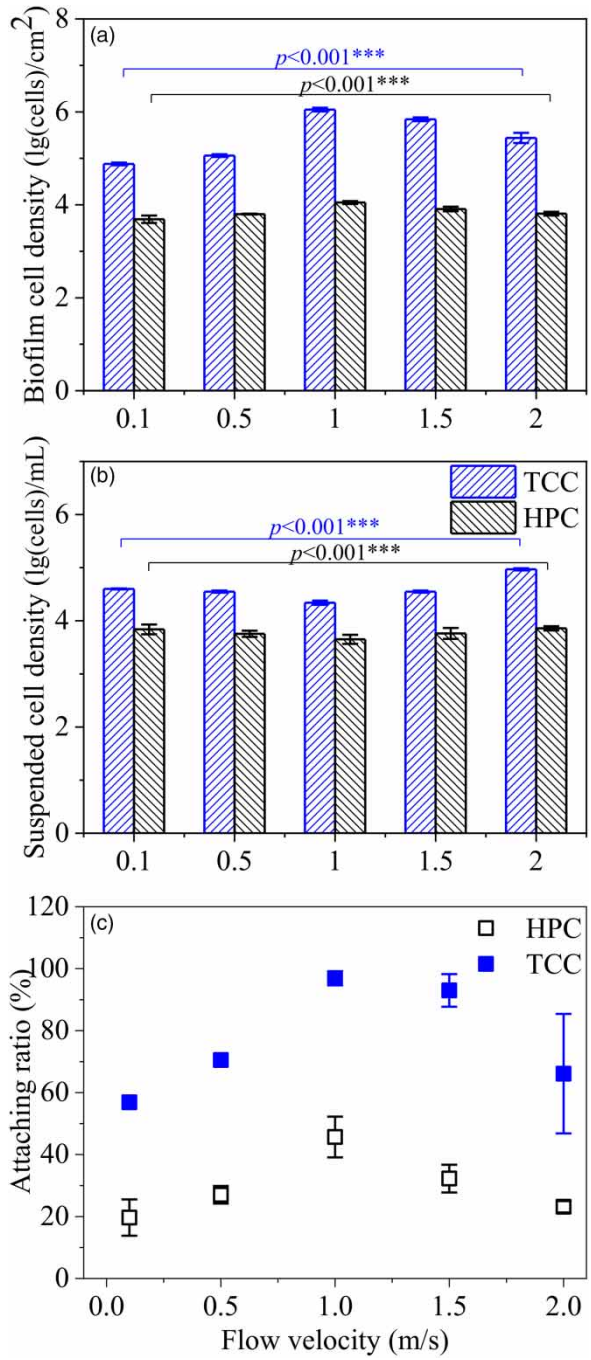

Figure 1 | (a) Biofilm cell density, (b) suspended cell density, and (c) the ratios of biofilm-embedded cells to total cells at 48 h after incubation under various flow velocities.

to 4.34 ± 0.04 lg(cells)/mL with the velocity increasing from 0.1 to 1.0 m/s and rising to 4.97 ± 0.02 lg(cells)/mL at 2.0 m/s (Figure 1(b)). It resulted in a similar pattern of the biofilm/total cells ratio as compared with that of biofilm cells, i.e., the TCC ratio increased significantly from 56.86% ± 1.02% at 0.1 m/s velocity to upwards of 96.91% ± 2.26% at 1.0 m/s, followed by an apparent reduction to 66.11% ± 19.29% at 2.0 m/s velocity (Figure 1(c)). Similarly, the intermediate velocity of 1.0 m/s also yielded the highest HPC attaching ratio of 45.67% ± 6.56%.

The results conformed to the previous observations of enhanced biofilm formation at elevated velocity within a certain range. For example, in both copper and plastic pipes, the biofilm cells increased with elevated flow rates up to 0.8 L/min in a pilot distribution system (Lehtola *et al.* 2006). As for stainless steel grades 304 and 316, higher velocities (0.96 m/s and 1.75 m/s) also yielded augmented viable and total cell counts of biofilms, associated with higher levels of extracellular polysaccharide, as compared with a lower rate of 0.32 m/s (Percival *et al.* 1999). *Pseudomonas fluorescens* was found to increase adhesive strength as the fluid velocity increased in the range of 0.6–1.6 m/s (Chen *et al.* 2005). This may be attributed to facilitated mass transport and excited bacterial activity at elevated flow velocity (Wang *et al.* 2014). Flow regimes could affect the formation and destination of aggregates that are crucial in seeding biofilm formation. Tsagkari *et al.* (2017) reported that aggregation was promoted in turbulent flow compared with laminar flow; inoculating with *Methylobacterium* further enhanced the aggregation. Tsagkari & Sloan (2018b) observed that different flow regimes resulted in substantial changes in biofilm morphology and growth and specifically the turbulent regime elevated both the initial formation and development of biofilms with the greatest roughness on the accessible surfaces compared with laminar and transition regimes. Instead of enhancing biofilm formation potentials, excessive shear forces at high velocities retarded bacterial activity and encouraged the detachment of biofilm cells, thereby contributing to reduced biofilm formation (Raya *et al.* 2010). In addition, Purevdorj *et al.* (2002) suggested that the dilution of signal molecules by mass transfer effects in faster flowing systems modified their influence on biofilm structure.

Effects of flow velocities on EPS secretion of biofilm and suspended cells

Evidence showed that nutrient limitation, toxic chemicals, hydrodynamic shear force and other stressful conditions could enhance microbial EPS production for self-protection (Flemming & Wingender 2010). After 48 h incubated in the experimental systems, the biofilms were collected and analyzed using a CLSM. As illustrated in Figure 2, the biofilms were dominated by EPS rather than cells (blue), while the EPS was predominantly composed of proteins (red) and α-polysaccharides (green) along with particularly sparse β-polysaccharides (yellow), regardless of hydrodynamic conditions. Interestingly, greater cell adhesion and more extensive EPS were observed for biofilms grown at 1.0 m/s velocity compared with those at lower (0.1 m/s) or higher (2.0 m/s) velocities.

To further quantify hydrodynamics-stressed EPS release and its impacts on biofilm formation in a DWDS environment, the EPS amounts (characterized in terms of PN and PS) at various flow velocities were analyzed, with results depicted in Figure 3. Statistically, flow velocity affected EPS production significantly ($p < 0.001$). With velocity increasing from 0.1 to 1.0 m/s, the shear-induced EPS release of biofilm cells at 48 h was observed with an increase of PN content from 8.99 ± 0.11 to 9.78 ± 0.09 μg/lg(cells) and of PS amount from 1.46 ± 0.09 to 1.64 ± 0.09 μg/lg(cells) (Figure 3(a)). In contrast, a decay in PN and PS production to 8.77 ± 0.21 and 1.13 ± 0.04 μg/lg(cells) was observed at 2.0 m/s velocity. The suspended cells experienced similar EPS variations as compared with biofilm cells in response to flow variations. During 48 h incubation, biofilm and suspended cells exhibited an analogous variation pattern to the PN and PS production rates, i.e., the rates increased and then decreased with velocity increasing, reaching peak PN and PS rates of 0.20 and 0.07 μg/lg(cells)·h for biofilm cells and 0.07 and 0.02 μg/lg(cells)·h for suspended cells at 1.0 m/s, respectively (Figure 3(b)). Our results revealed that the intermediate velocity level (1.0 m/s) considerably promoted EPS production, while at high velocity levels, inhibition of cell activity reduced EPS release.

Statistical analysis showed a positive correlation between EPS amounts of biofilm and attaching ratios ($r = 0.88$, $p < 0.05$) reflecting favored surface aggregation

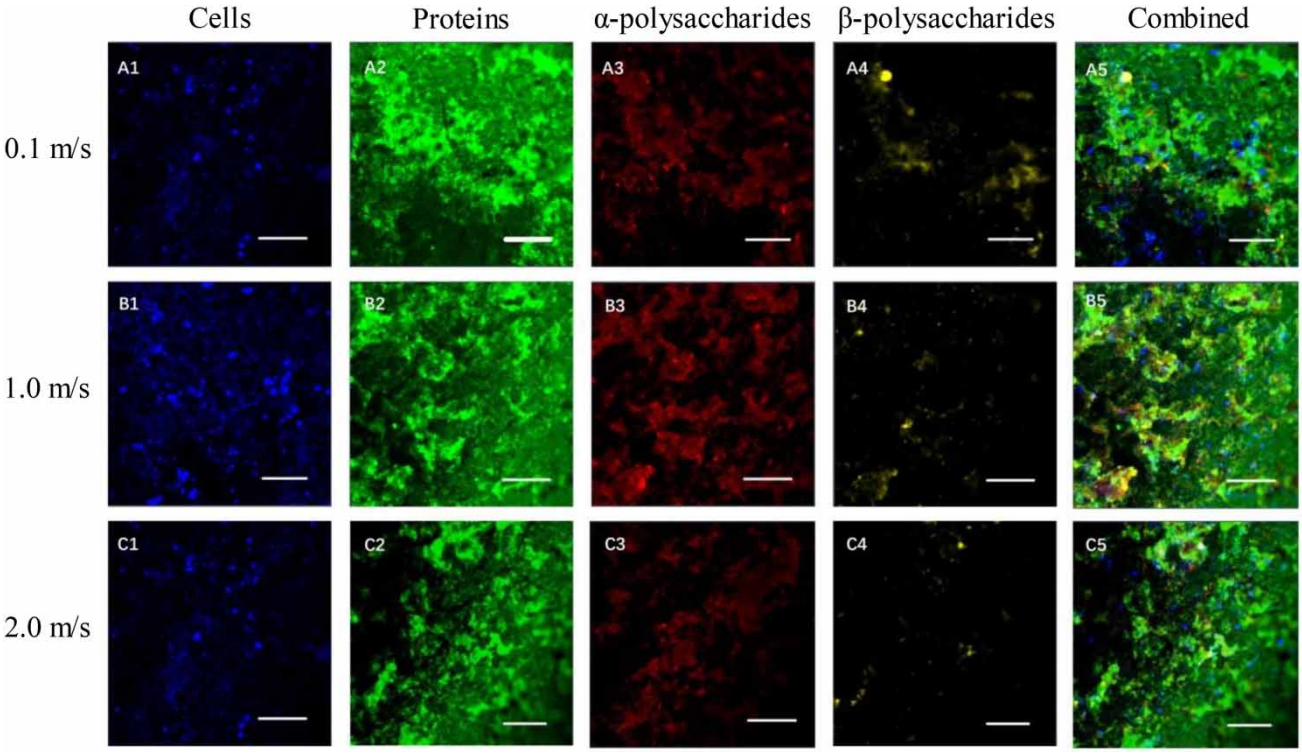

Figure 2 | CLSM images of biofilm cells and EPS distributions after 48 h incubation at flow velocities of 0.1, 1.0 and 2.0 m/s. (A1, B1, C1) CLSM images of total cells (blue, SYTO 63), (A2, B2, C2) CLSM images of protein (green, FITC), (A3, B3, C3) CLSM images of α-polysaccharide (red, ConA), (A4, B4, C4) CLSM images of β-polysaccharide (yellow, calcofluor white), and (A5, B5, C5) combined images, scale bar: 50 μm. Please refer to the online version of this paper to see this figure in color: http://dx.doi.org/10.2166/ws.2020.039.

by EPS production at intermediate velocity in DWDS. The mechanism of environment-stressed EPS production shaping cell–surface interactions and thereby surface aggregation is consistent with previous reports of pure culture conditions and a two-species system. For instance, Ducret *et al.* (2012) reported that slime secretion of gliding *Myxococcus xanthus* cells was associated preferentially with the outermost components of the motility machinery and promoted cell adhesion to the substrate. For the photosynthetic bacterium *Chloroflexus aggregans*, extracellular protease secreted from *Bacillus licheniformis* mediated interspecies interaction and encouraged its aggregation (Morohoshi *et al.* 2015).

Zeta potential and hydrophobicity of suspended cells under various hydrodynamic conditions

Surface potential and hydrophobicity are generally considered the triggering forces for surface adhesion. Figure 4 depicts the zeta potentials and hydrophobicity of suspended cells 48 h after inoculation. With velocity elevating from 0.1 to 1.0 m/s, zeta potential value decreased from 17.34 ± 1.02 to 11.62 ± 1.57 -mV, accompanied with hydrophobicity boosting from $52.90\% \pm 4.38\%$ to $58.16\% \pm 2.19\%$. Interestingly, a continuous elevation to 2.0 m/s yielded an ascending zeta potential back to 17.60 ± 0.62 -mV associated with a hydrophobicity of $37.54\% \pm 2.50\%$. For suspended cells, zeta potential and EPS amounts were negatively correlated with a coefficient of -0.986 ($p < 0.01$), albeit a positive moderate correlation between surface hydrophobicity and EPS contents ($r = 0.729$). Similarly, a higher negative charge density was found to be linked to the reduced production of PS and PN induced by D-tyrosine (Xu & Liu 2011). Cell-surface-attached EPS components encompassing an assortment of usually charged functional groups could considerably impact the physicochemical properties of cell surfaces (Tielen *et al.* 2010; Das *et al.* 2011).

A direct negative correlation between zeta potential and attaching ratio ($r = -0.928$, $p < 0.05$) was found at various velocities. The lower zeta potential associated with

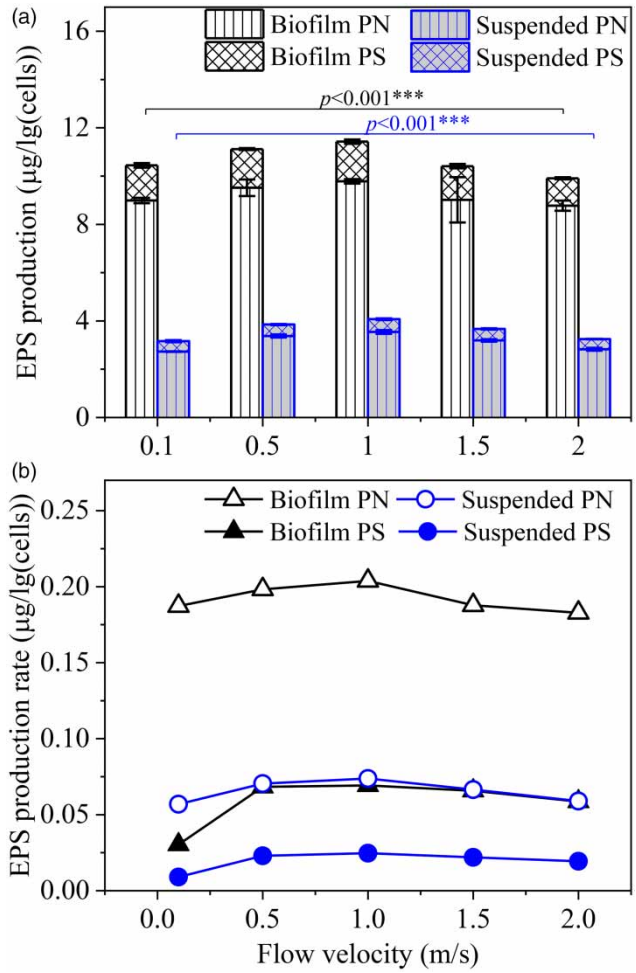

Figure 3 | EPS production of (a) biofilm-embedded and (b) suspended cells at 48 h after incubation under various flow velocities.

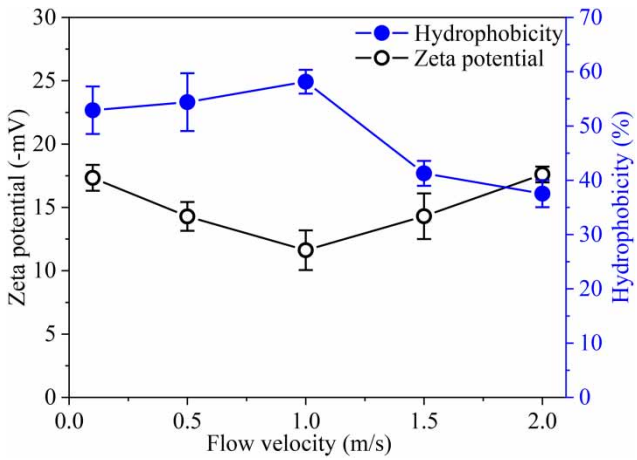

Figure 4 | Zeta potential and hydrophobicity of suspended cells at 48 h after incubation under various flow velocities.

augmented EPS production corresponded to enhanced biofilm formation at intermediate flow velocity, reminiscent of the classical DLVO theory that suppression of electrorepulsive forces facilitated cell–cell and cell–surface interactions (Zita & Hermansson 1994). Consideration of augmented hydrophobicity provides an alternative explanation for promoted adhesion behavior at intermediate flow velocity. Previous studies reported that presence of naturally produced extracellular DNA on both Gram-negative and Gram-positive bacterial cell surfaces affected surface hydrophobicity and promoted attractive acid–base interactions between cells and surfaces (Das *et al.* 2010, 2011).

Bacterial community of biofilms developed under various hydrodynamic conditions

The Shannon diversity index for biofilm bacterial communities revealed a community shift from high (2.45) to low (1.70) diversity at velocities from 0.1 to 1.0 m/s followed by an increase in diversity (4.47) at 2.0 m/s velocity. It suggests that DWDS bacterial diversity could be lowered by intermediate flow velocity (1.0 m/s). The high diversity at lower or higher velocity (lower flux or higher shear stress) indicates a high metabolic versatility of bacterial communities, which would allow them harsh-environment adaptation (Lautenschlager *et al.* 2014). Meanwhile, surface colonization was lowered accompanying such uneven community. Accordingly, the existence of a higher diverse community may lead to higher functional stability confronting environmental stresses (Wittebolle *et al.* 2009).

Shifts in biofilm bacterial community were recorded under various velocities at phylum level (Figure 5). *Proteobacteria* dominated within all sampled biofilm community, and has been repeatedly detected as predominant in drinking water systems (Williams *et al.* 2004; Lautenschlager *et al.* 2014; Lin *et al.* 2014). The abundance of this phylum increased from 55.11% to 78.16% with the velocity rising from 0.1 to 1.0 m/s followed by a decrease to 62.78% at 2.0 m/s. It suggests that intermediate velocity stimulates the dominance of *Proteobacteria* in a DWDS. The second abundant phylum was *Actinobacteria*, accounting for 42.27%, 20.62% and 32.31% at the velocities of 0.5, 1.0 and 1.5 m/s, respectively, while *Firmicutes* occupied the second large phylum with a content of 37.50% at 0.1 m/s

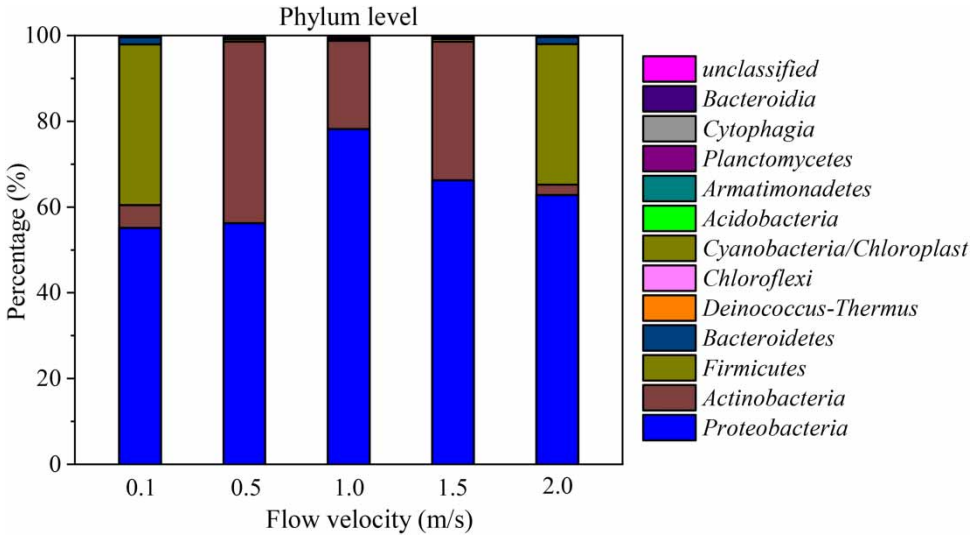

Figure 5 | Relative abundance of bacterial species attached to pipes at phylum level at 48 h after incubation under different velocities.

and of 32.78% at 2.0 m/s. Sampling from an urban water distribution system in Greece, Kormas *et al.* (2010) observed that *Proteobacteria* dominated in the bacterial community of the water samples collected from pumping wells and water treatment tanks, while *Actinobacteria* was detected as predominant in household waters. Figure 6 depicts the variability of biofilm composition at genus level along with hydrodynamics fluctuations. Specifically, *Pseudomonas* (24.13%), *Rhodococcus* (19.49%) and *Aquabacterium* (15.05%) were the most dominating groups at 0.1 m/s velocity. Confronting 1.0 m/s flow environment, the major groups changed to *Pseudomonas* (37.69%) and *Rhodococcus* (32.17%). In contrast, *Rhodococcus* (41.95%) was dominant followed by *Pseudomonas* (29.31%) in the biofilm compositions at 2.0 m/s velocity. Overall, *Pseudomonas* was the genus dominant in the composition of most sampled

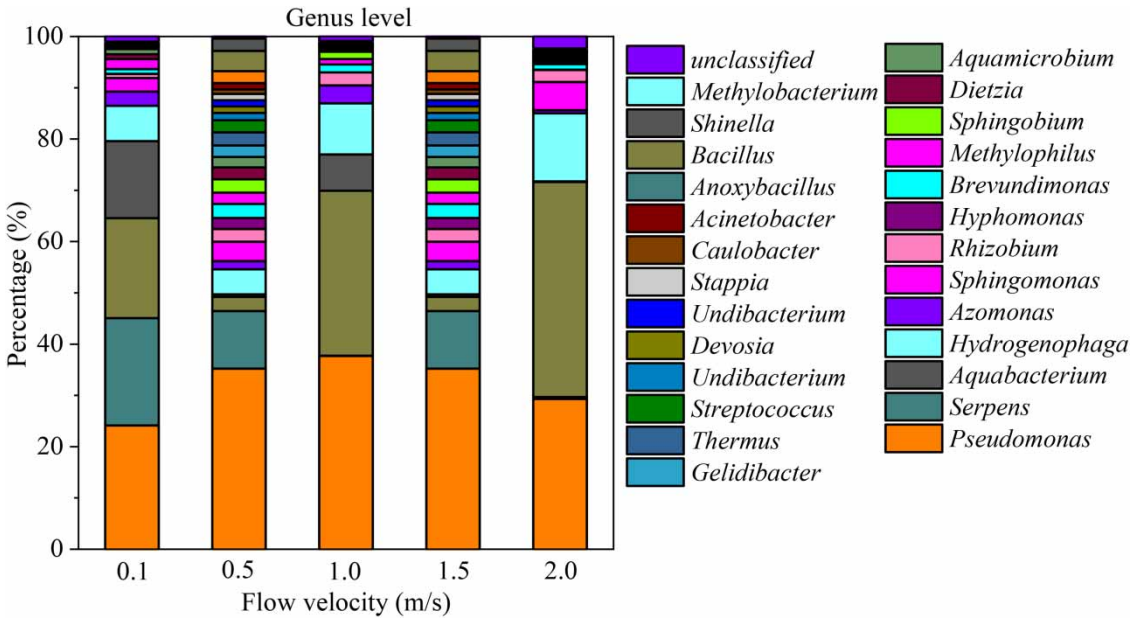

Figure 6 | Relative abundance of bacterial species attached to pipes at genus level at 48 h after incubation under different velocities.

biofilms, particularly at 1.0 m/s velocity. These species have higher capacity to form biofilm due to their enhanced ability of EPS secretion, thereby favoring biofilm formation (Douterelo *et al.* 2014). Cyclic patterns in planktonic composition have been observed associated with hydrodynamics fluctuations in a small, looped water distribution system (Sekar *et al.* 2012). Douterelo *et al.* (2014) suggested similar planktonic species were involved in the process of surface attachment and initial biofilm formation.

CONCLUSIONS

Results showed that intermediate velocity (1.0 m/s) yielded increasing biofilm cells, associated with enhanced EPS production. Correlation between EPS release, zeta potential and hydrophobicity of suspended cells suggested that EPS release might alter surface properties, thus affecting microbial aggregation onto pipe surfaces. Shifts in biofilm bacterial community were observed along with hydrodynamics fluctuations. *Proteobacteria* and *Actinobacteria* dominated the biofilm samples incubated at the velocities of 0.5, 1.0 and 1.5 m/s, while *Proteobacteria* and *Firmicutes* were the most abundant at 0.1 and 2.0 m/s after 48 h incubation. *Pseudomonas* was the genus predominant in the composition of most sampled biofilms, particularly at 1.0 m/s velocity. Overall, this study offers insights into microbial responses and the mechanistic understanding of biofilm dynamics populating the hydrodynamically fluctuating DWDS environment.

ACKNOWLEDGMENTS

This study was financially supported by the Natural Science Foundation of China (51479046) and the National Key Research and Development Program of China (2016YFC0401303).

SUPPLEMENTARY MATERIAL

The Supplementary Material for this paper is available online at https://dx.doi.org/10.2166/ws.2020.039.

REFERENCES

Bertelli, C., Courtois, S., Rosikiewicz, M., Piriou, P., Aeby, S., Robert, S., Loret, J.-F. & Greub, G. 2018 Reduced chlorine in drinking water distribution systems impacts bacterial biodiversity in biofilms. *Frontiers in Microbiology* **9** (10), 2520.

Chen, M. J., Zhang, Z. & Bott, T. R. 2005 Effects of operating conditions on the adhesive strength of *Pseudomonas fluorescens* biofilms in tubes. *Colloids and Surfaces B: Biointerfaces* **43** (2), 61–71.

Chen, M. Y., Lee, D. J. & Tay, J. H. 2007 Distribution of extracellular polymeric substances in aerobic granules. *Applied Microbiology and Biotechnology* **73** (6), 1463–1469.

Das, T., Sharma, P. K., Busscher, H. J., van der Mei, H. C. & Krom, B. P. 2010 Role of extracellular DNA in initial bacterial adhesion and surface aggregation. *Applied and Environmental Microbiology* **76** (10), 3405–3408.

Das, T., Krom, B. P., van der Mei, H. C., Busscher, H. J. & Sharma, P. K. 2011 DNA-mediated bacterial aggregation is dictated by acid–base interactions. *Soft Matter* **7** (6), 2927–2935.

Douterelo, I., Sharpe, R. L. & Boxall, J. B. 2012 Influence of hydraulic regimes on bacterial community structure and composition in an experimental drinking water distribution system. *Water Research* **47** (2), 503–516.

Douterelo, I., Sharpe, R. & Boxall, J. 2014 Bacterial community dynamics during the early stages of biofilm formation in a chlorinated experimental drinking water distribution system: implications for drinking water discolouration. *Journal of Applied Microbiology* **117**, 286–301.

Douterelo, I., Jackson, M., Solomon, C. & Boxall, J. 2016 Microbial analysis of in situ biofilm formation in drinking water distribution systems: implications for monitoring and control of drinking water quality. *Applied Microbiology and Biotechnology* **100** (7), 3301–3311.

Ducret, A., Valignat, M.-P., Mouhamar, F., Mignot, T. & Theodoly, O. 2012 Wet-surface–enhanced ellipsometric contrast microscopy identifies slime as a major adhesion factor during bacterial surface motility. *Proceedings of the National Academy of Sciences* **109** (25), 10036–10041.

Fish, K., Osborn, A. M. & Boxall, J. B. 2017 Biofilm structures (EPS and bacterial communities) in drinking water distribution systems are conditioned by hydraulics and influence discolouration. *Science of the Total Environment* **593–594**, 571–580.

Flemming, H.-C. & Wingender, J. 2010 The biofilm matrix. *Nature Reviews Microbiology* **8** (9), 623–633.

Guasto, J. S., Rusconi, R. & Stocker, R. 2012 Fluid mechanics of planktonic microorganisms. *Annual Review of Fluid Mechanics* **44** (1), 373–400.

Harshey, R. M. 2003 Bacterial motility on a surface: many ways to a common goal. *Annual Review of Microbiology* **57**, 249–273.

Jiang, B. & Liu, Y. 2013 Dependence of structure stability and integrity of aerobic granules on ATP and cell communication. *Applied Microbiology and Biotechnology* **97** (11), 5105–5112.

Kim, M. K., Ingremeau, F., Zhao, A., Bassler, B. L. & Stone, H. A. 2016 Local and global consequences of flow on bacterial quorum sensing. *Nature Microbiology* **1**, 15005.

Kirisits, M. J., Margolis, J. J., Purevdorj-Gage, B. L., Vaughan, B., Chopp, D. L., Stoodley, P. & Parsek, M. R. 2007 Influence of the hydrodynamic environment on quorum sensing in *Pseudomonas aeruginosa* biofilms. *Journal of Bacteriology* **189** (22), 8357–8360.

Kormas, K. A., Neofitou, C., Pachiadaki, M. & Koufostathi, E. 2010 Changes of the bacterial assemblages throughout an urban drinking water distribution system. *Environmental Monitoring and Assessment* **165**, 27–38.

Lautenschlager, K., Hwang, C., Ling, F., Liu, W. T., Boon, N., Köster, O., Egli, T. & Hammes, F. 2014 Abundance and composition of indigenous bacterial communities in a multi-step biofiltration-based drinking water treatment plant. *Water Research* **62**, 40–52.

LeChevallier, M. W., Cawthon, C. D. & Lee, R. G. 1988 Factors promoting survival of bacteria in chlorinated water supplies. *Applied and Environmental Microbiology* **54** (3), 649–654.

Lehtola, M. J., Miettinen, I. T., Keinänen, M. M., Kekki, T. K., Laine, O., Hirvonen, A., Vartiainen, T. & Martikainen, P. J. 2004 Microbiology, chemistry and biofilm development in a pilot drinking water distribution system with copper and plastic pipes. *Water Research* **38** (17), 3769–3779.

Lehtola, M. J., Laxander, M., Miettinen, I. T., Hirvonen, A., Vartiainen, T. & Martikainen, P. J. 2006 The effects of changing water flow velocity on the formation of biofilms and water quality in pilot distribution system consisting of copper or polyethylene pipes. *Water Research* **40** (11), 2151–2160.

Lemos, M., Gomes, I., Mergulhão, F., Melo, L. & Simões, M. 2015 The effects of surface type on the removal of *Bacillus cereus* and *Pseudomonas fluorescens* single and dual species biofilms. *Food and Bioproducts Processing* **93**, 234–241.

Li, X. Y. & Yang, S. F. 2007 Influence of loosely bound extracellular polymeric substances (EPS) on the flocculation, sedimentation and dewaterability of activated sludge. *Water Research* **41** (5), 1022–1030.

Lin, W., Yu, Z., Zhang, H. & Thompson, I. P. 2014 Diversity and dynamics of microbial communities at each step of treatment plant for potable water generation. *Water Research* **52**, 218–230.

Liu, Y. & Tay, J.-H. 2002 The essential role of hydrodynamic shear force in the formation of biofilm and granular sludge. *Water Research* **36**, 1653–1665.

Liu, L., Hu, Q., Le, Y., Chen, G., Tong, Z., Xu, Q. & Wang, G. 2017 Chlorination-mediated EPS excretion shapes early-stage biofilm formation in drinking water systems. *Process Biochemistry* **55**, 41–48.

Lorite, G. S., de Souza, A. A., Neubauer, D., Mizaikoff, B., Kranz, C. & Cotta, M. A. 2013 On the role of extracellular polymeric substances during early stages of *Xylella fastidiosa* biofilm formation. *Colloids and Surfaces B: Biointerfaces* **102**, 519–525.

Manuel, C. M., Nunes, O. C. & Melo, L. F. 2007 Dynamics of drinking water biofilm in flow/non-flow conditions. *Water Research* **41**, 551–562.

Morohoshi, S., Matsuura, K. & Haruta, S. 2015 Secreted protease mediates interspecies interaction and promotes cell aggregation of the photosynthetic bacterium *Chloroflexus aggregans*. *FEMS Microbiology Letters* **362** (3), 1–5.

O'Toole, G. A. & Kolter, R. 1998 Flagellar and twitching motility are necessary for *Pseudomonas aeruginosa* biofilm development. *Molecular Microbiology* **30** (2), 295–304.

Percival, S. L., Knapp, J. S., Edyvean, R. & Wales, D. S. 1998 Biofilm development on stainless steel in mains water. *Water Research* **32** (1), 243–253.

Percival, S. L., Knapp, J. S., Wales, D. S. & Edyvean, R. G. J. 1999 The effect of turbulent flow and surface roughness on biofilm formation in drinking water. *Journal of Industrial Microbiology & Biotechnology* **22**, 152–159.

Picioreanu, C., Kreft, J.-U., Klausen, M., Haagensen, J. A. J., Tolker-Nielsen, T. & Molin, S. 2007 Microbial motility involvement in biofilm structure formation – a 3D modelling study. *Water Science & Technology* **55** (8–9), 337–343.

Potgieter, S., Pinto, A., Sigudu, M., du Preez, H., Ncube, E. & Venter, S. 2018 Long-term spatial and temporal microbial community dynamics in a large-scale drinking water distribution system with multiple disinfectant regimes. *Water Research* **139**, 406–419.

Pratt, L. A. & Kolter, R. 1998 Genetic analysis of *Escherichia coli* biofilm formation: roles of flagella, motility, chemotaxis and type I pili. *Molecular Microbiology* **30** (2), 285–293.

Purevdorj, B., Costerton, J. W. & Stoodley, P. 2002 Influence of hydrodynamics and cell signaling on the structure and behavior of *Pseudomonas aeruginosa* biofilms. *Applied and Environmental Microbiology* **68** (9), 4457–4464.

Raya, A., Sodagari, M., Pinzon, N. M., He, X., Newby, B. M. Z. & Ju, L. K. 2010 Effects of rhamnolipids and shear on initial attachment of *Pseudomonas aeruginosa* PAO1 in glass flow chambers. *Environmental Science and Pollution Research* **17** (9), 1529–1538.

Rochex, A., Godon, J.-J., Bernet, N. & Escudié, R. 2008 Role of shear stress on composition, diversity and dynamics of biofilm bacterial communities. *Water Research* **42** (20), 4915–4922.

Rosenberg, M., Gutnick, D. & Rosenberg, E. 1980 Adherence of bacteria to hydrocarbons: a simple method for measuring cell-surface hydrophobicity. *FEMS Microbiology Letters* **9**, 29–33.

Sekar, R., Deines, P., Machell, J., Osborn, A. M., Biggs, C. A. & Boxall, J. B. 2012 Bacterial water quality and network hydraulic characteristics: a field study of a small, looped water distribution system using culture-independent molecular methods. *Journal of Applied Microbiology* **112**, 1220–1234.

Shen, Y., Monroy, G. L., Derlon, N., Janjaroen, D., Huang, C., Morgenroth, E., Boppart, S. A., Ashbolt, N. J., Liu, W.-T. & Nguyen, T. H. 2015 Role of biofilm roughness and hydrodynamic conditions in *Legionella pneumophila* adhesion to and detachment from simulated drinking water

biofilms. *Environmental Science and Technology* **49** (7), 4274–4282.

Simões, M., Pereira, M. O., Sillankorva, S., Azeredo, J. & Vieira, M. J. 2007 The effect of hydrodynamic conditions on the phenotype of *Pseudomonas fluorescens* biofilms. *Biofouling* **23** (4), 249–258.

Soini, S. M., Koskinen, K. T., Vilenius, M. J. & Puhakka, J. A. 2002 Effects of fluid-flow velocity and water quality on planktonic and sessile microbial growth in water hydraulic system. *Water Research* **36** (15), 3812–3820.

Srinivasan, S., Harrington, G. W., Xagoraraki, I. & Goel, R. 2008 Factors affecting bulk to total bacteria ratio in drinking water distribution systems. *Water Research* **42**, 3393–3404.

Stoodley, P., Dodds, I., Boyle, J. D. & Lappin-Scott, H. M. 1999 Influence of hydrodynamics and nutrients on biofilm structure. *Journal of Applied Microbiology* **85** (S1), 19S–28S.

Teodósio, J. S., Simões, M., Melo, L. F. & Mergulhão, F. J. 2011 Flow cell hydrodynamics and their effects on *E. coli* biofilm formation under different nutrient conditions and turbulent flow. *Biofouling* **27** (1), 1–11.

Tielen, P., Rosenau, F., Wilhelm, S., Jaeger, K.-E., Flemming, H.-C. & Wingender, J. 2010 Extracellular enzymes affect biofilm formation of mucoid *Pseudomonas aeruginosa*. *Microbiology* **156** (7), 2239–2252.

Tsagkari, E. & Sloan, W. T. 2018a The role of the motility of *Methylobacterium* in bacterial interactions in drinking water. *Water* **10** (10), 1386.

Tsagkari, E. & Sloan, W. T. 2018b Turbulence accelerates the growth of drinking water biofilms. *Bioprocess and Biosystems Engineering* **41**, 757–770.

Tsagkari, E., Keating, C., Couto, J. M. & Sloan, W. T. 2017 A keystone *Methylobacterium* strain in biofilm formation in drinking water. *Water* **9** (10), 778.

Wang, C., Miao, L., Hou, J., Wang, P., Qian, J. & Dai, S. 2014 The effect of flow velocity on the distribution and composition of extracellular polymeric substances in biofilms and the detachment mechanism of biofilms. *Water Science and Technology* **69** (4), 825–832.

Williams, M. M., Domingo, J. W. S., Meckes, M. C., Kelty, C. A. & Rochon, H. S. 2004 Phylogenetic diversity of drinking water bacteria in a distribution system simulator. *Journal of Applied Microbiology* **96**, 954–964.

Wittebolle, L., Marzorati, M., Clement, L., Balloi, A., Daffonchio, D., Heylen, K., De Vos, P., Verstraete, W. & Boon, N. 2009 Initial community evenness favours functionality under selective stress. *Nature* **458** (7238), 623–626.

Xu, H. & Liu, Y. 2011 Reduced microbial attachment by D-amino acid-inhibited AI-2 and EPS production. *Water Research* **45** (17), 5796–5804.

Zacheus, O. M., Lehtola, M. J., Korhonen, L. K. & Martikainen, P. J. 2001 Soft deposits, the key site for microbial growth in drinking water distribution networks. *Water Research* **35** (7), 1757–1765.

Zhang, J., Li, W., Chen, J., Qi, W., Wang, F. & Zhou, Y. 2018 Impact of biofilm formation and detachment on the transmission of bacterial antibiotic resistance in drinking water distribution systems. *Chemosphere* **203**, 368–380.

Zita, A. & Hermansson, M. 1994 Effects of ionic strength on bacterial adhesion and stability of flocs in a wastewater activated sludge system. *Applied and Environmental Microbiology* **60** (9), 3041–3048.

First received 25 November 2019; accepted in revised form 28 February 2020. Available online 16 March 2020